Cyclone-Scale Forcing of Ultralong Waves

ROBERT GALL AND RICHARD BLAKESLEE

Institute of Atmospheric Physics, The University of Arizona, Tucson, AZ 85721

RICHARD C. J. SOMERVILLE

National Center for Atmospheric Research[1], Boulder, CO 80307

(Manuscript received 26 December 1978; in final form 4 May 1979)

ABSTRACT

A numerical experiment is carried out with a simplified general circulation model. In this experiment, instabilities of all wavelengths are allowed to develop simultaneously from small perturbations on a zonally symmetric flow. The initial development of the ultralong waves in this experiment is apparently forced by the interaction between the cyclone-scale waves and the basic flow in which they are embedded. Because the spectrum of the developing baroclinic waves is not monochromatic, the interaction between the cyclones and the basic flow varies with longitude, and waves longer than the cyclone scale are forced. The structure of the ultralong waves in the numerical experiment is consistent with this forcing mechanism. One implication for numerical weather prediction is that errors in forecasts of ultralong waves may be due in part to errors in the cyclone scale.

1. Introduction

Several distinct processes might conceivably play a role in forcing the development of the transient ultralong waves (zonal wavenumbers 1–4) of the middle-latitude general circulation. One is simply baroclinic instability of the basic zonal current. Hirota (1968) has shown that when this basic current is assumed to be invariant with latitude, the ultralong waves are indeed unstable, and the structure of these unstable waves resembles that of the ultralong waves observed in the atmosphere. However, the growth rate of the ultralong waves in Hirota's model (<0.1 day^{-1}) is quite small when compared to the growth rate of the fastest growing baroclinic waves (>0.5 day^{-1}). Subsequent work by Song (1971) and Brown (1969) indicated that if at least some of the horizontal variation in the basic flow is taken into account, the ultra-long waves are still unstable, although the instability is primarily barotropic. However, as in Hirota's model, the growth rates are again much less than the growth rates of the baroclinic waves with wavenumbers >7.

More recently, Gall (1976a) and Simmons and Hoskins (1977) have examined the stability of realistic zonal flows on the sphere. They also found very small growth rates for the ultralong waves, although the energy source could be either baroclinic or barotropic, depending on the details of the structure of the zonal flow. It would thus appear that if the ultralong waves were forced primarily by the instability of the zonal flow, they would grow at much slower rates than the fastest growing baroclinic waves.

Another manner in which the ultralong waves might be forced is through nonlinear interwave interactions which transfer energy into the ultralong waves from other portions of the spectrum. Kinetic energy entering the spectrum through baroclinic instability at wavenumbers near 7 is in part transferred to longer wavelengths by nonlinear interactions (e.g., Kraichnan, 1967; Lilly, 1969; Charney, 1971). A similar process occurs in a two-dimensional fluid with energy generation in a narrow spectral range.

In a companion paper (Gall *et al.*, 1979), we have described two numerical experiments in which a general circulation model (GCM) is used to simulate the development of waves as they grow from small perturbations on an initial flow that is zonally constant. In those experiments the initial perturbations of the ultralong waves actually decayed for the first 10 days, during which time the waves in the portion of the spectrum growing by baroclinic instability (wavenumbers 5–20) amplified exponentially. After the baroclinic waves had undergone significant amplification, the ultralong waves began to develop rapidly and, in fact, achieved growth rates *exceeding* those of the baroclinic

[1] The National Center for Atmospheric Research is sponsored by the National Science Foundation.

0022-4928/79/091692-07$05.75

waves. Similar behavior of the ultralong waves is also apparent in earlier numerical experiments (Gall, 1976b).

The tendency for the ultralong waves to decay during the first 10 days indicates that frictional processes dominate any energy sources for the waves, including sources due to the instability of these waves on the zonal flow. This behavior is consistent with the stability studies cited earlier, which suggest that in the absence of frictional processes the growth rate of the ultralong waves is very small. Inclusion of frictional processes in the numerical experiments apparently reduces this growth rate still further. Additionally, the linear instability of wavenumber 3 on the zonal flow was found to decrease with time. Therefore, the later development of this wave cannot be related directly to baroclinic or barotropic instability.

The developing ultralong waves might be expected first to decay and then to amplify rapidly as the baroclinic waves reach large amplitude, if their development is forced by the nonlinear transfer of energy from the waves growing by baroclinic instability. However, an examination of the energy budget for these waves shows that the primary kinetic energy source for wavenumbers 1–4 is the conversion from wave available potential energy to wave kinetic energy at a given wavenumber, and not nonlinear energy transfer between the various wavenumbers. Although this latter energy source is significant for these waves, the baroclinic energy source is at least twice as large, except for wavenumber 1. It would thus appear that the mechanism that forces the ultralong waves is not strictly due to any of the processes outlined above.

Of course, these mechanisms do not exhaust the possibilities. In the following discussion, we describe and explain qualitatively the development of the baroclinic waves and the ultralong waves in our numerical experiment. For this purpose, we employ a simple physical argument which seems consistent with the numerical results and which may have heuristic value, although it is quite speculative. This argument leads to the conclusion that the ultralong waves early in these experiments are forced by interactions between the growing cyclones and the basic flow in which the cyclones are embedded. Here we use the term "basic flow" to refer to the flow averaged zonally over a restricted domain, such as the wavelength of one cyclone or one baroclinic wave, in contrast to "zonal flow" which implies averaging around an entire latitude circle.

We shall refer to an experiment that has been discussed in more detail by Gall *et al.* (1979). Experiment 1, as it was denoted, consisted of a 25-day integration of a simplified general circulation model in which the initial conditions were zonally

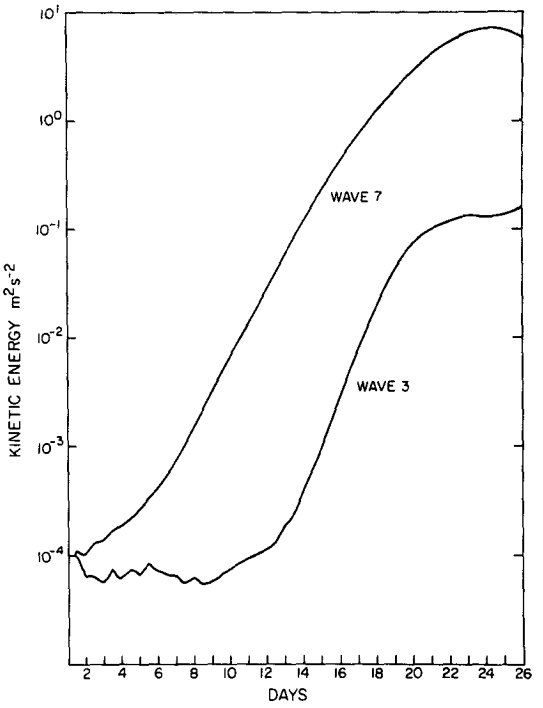

FIG. 1. The kinetic energy of wavenumbers 7 and 3 as a function of time in the numerical experiment. Day 1 is the initial condition.

constant except for small random perturbations in the pressure field. The model was the second-generation NCAR GCM, described by Oliger *et al.* (1970), Kasahara and Washington (1971) and Washington and Williamson (1977). The horizontal resolution was 2.5° and the vertical resolution was 3 km, with a top at 18 km. During the integration, parameterizations of diabatic processes involving the release of latent heat, sensible heat transfer with the earth's surface and radiation were removed from the model. In addition, mountains were not included, and the computational domain was the Northern Hemisphere.

2. Results

a. Energetics

Fig. 1 shows the development of kinetic energy in waves 7 and 3 in the experiment. The behavior of wave 7 is straightforward. There is a long period of exponential growth starting almost at Day 1, followed by a period of decreasing growth rate and then a slow decay.

Wave 3, on the other hand, decays for the first 10 days but then develops exponentially after Day 10 and actually achieves a growth rate greater than that of wave 7. In this experiment the maximum growth rate achieved by wave 3 was at least 30% greater than the maximum growth rate achieved by the fastest growing baroclinic waves.

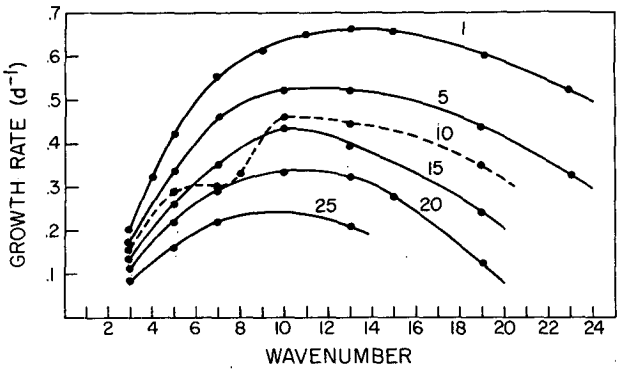

FIG. 2. Linear inviscid growth rate spectrum for the zonal flow of the experiment as a function of time. The numbers denote time in days from the beginning of the experiment. Day 1 is the initial condition.

Fig. 2 (from Gall *et al.*, 1979) demonstrates that the rapid growth of wavenumber 3 after Day 10 is not due to baroclinic or barotropic instability. This figure shows the linear inviscid growth rate spectrum of the zonal flow at selected times during the integration. The inviscid growth rate of wave 3 is always small but positive, and it decreases monotonically with time. Since wave 3 decayed for the first 10 days, the sources of energy for wave growth at the beginning of the experiment, represented by the linear inviscid growth rate, are apparently more than offset by dissipation. Hence, the wave is stable in the sense of classical baroclinic or barotropic instability of the zonal flow. Furthermore, because the linear inviscid growth rate decreases with time throughout the experiment, the sudden growth of wave 3 after Day 10 is clearly not the result of an increase in the baroclinic/barotropic instability of the zonal flow due to nonlinear interactions.

The lower part of Fig. 3 shows the energy budget for wave 3, normalized by the kinetic energy of the wave. The calculation of this energy budget is described by Baker *et al.* (1977, 1978). Although energy is supplied to the wave by other wavelengths through $L(n)$, as is predicted by two-dimensional turbulence theory (Fjortoft, 1953), there is a lengthy period starting about Day 7 during which most of the energy is supplied by baroclinic processes. The upper part of Fig. 3 also shows that for wave 1, $C(n)$ exceeds $L(n)$ for the main part of the experiment. Therefore, even though these ultralong waves are only weakly unstable on the zonal flow, they are nevertheless growing principally by baroclinic processes early in the experiment.

b. Synoptics

The mechanism that forces the development of the ultralong wave in these experiments can apparently be explained qualitatively using very simple arguments. The cyclones, which are the synoptic manifestation of the portion of the spectrum that is growing by baroclinic instability, are of varying intensity around a latitude circle. This is because the developing spectrum is not monochromatic but is rather broad and contains a number of spikes. It is thus not surprising to find a variation of the intensity of the cyclones on length scales much longer than that of the cyclones themselves.

Fig. 4 shows the distribution of surface pressure at Day 18.5 from Experiment 1 of Gall *et al.* (1979). There are eight cyclones of comparable horizontal scale, and the minimum pressure of these cyclones varies by 4 mb or about 30% of the average pressure difference between adjacent highs and lows. Regions of stronger and weaker cyclones are spaced non-

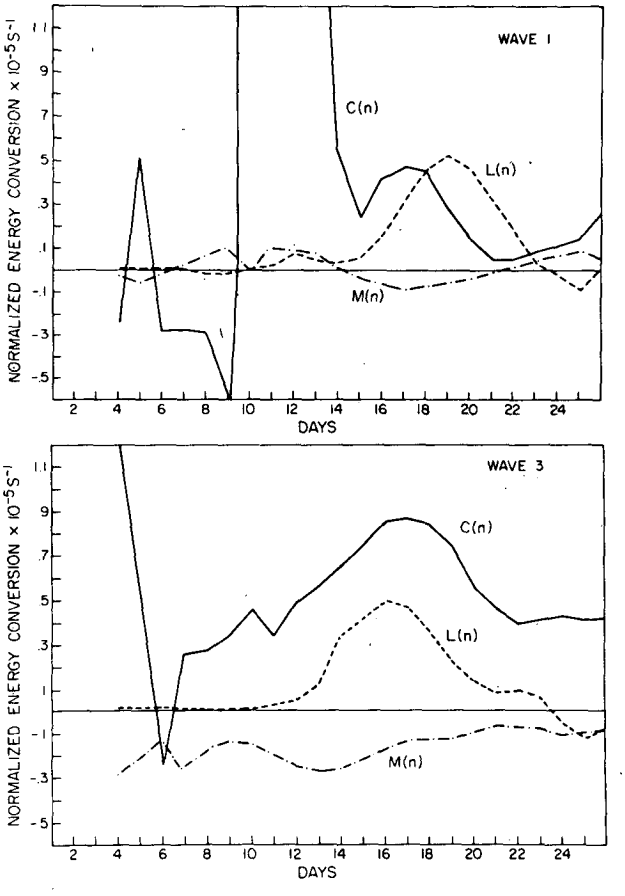

FIG. 3. The time variation of $M(n)$, the conversion of kinetic energy from wavenumber n to the kinetic energy of the zonal flow; $C(n)$, the conversion of available potential energy to kinetic energy within wavenumber n; and $L(n)$, the transfer of kinetic energy from all other wavenumbers to the kinetic energy of wavenumber n, for wave 1 (top) and wave 3 (bottom). Data are normalized by the total kinetic energy of the wave.

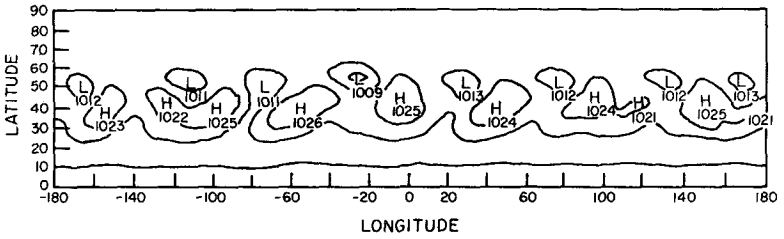

FIG. 4. Distribution of surface pressure at Day 18.5. Central pressures (mb) are shown.

uniformly around the hemisphere at about the same latitude (50°N). Thus, the variation in the intensity of the cyclones involves length scales longer than those of the cyclones themselves. As these cyclones intensify, they begin to interact with the basic flow, and it is this nonlinear interaction between the developing cyclones and the basic state in which they are embedded that apparently forces the initial development of the ultralong waves.

The upper portion of Fig. 5 illustrates schematically that if the cyclones are of equal intensity around the globe, all the cyclones will transport heat northward at the same rate, producing a modification of the temperature field north (south) of the cyclones due to the convergence (divergence) of the eddy heat flux in these regions. With no longitudinal variation in the eddy heat flux, only the zonal mean component of temperature will be modified. An extreme situation, with cyclones confined to only a section of the globe, is depicted in the lower portion of Fig. 5. In this case, the temperatures will be modified by the eddy heat flux only in small regions near the cyclones. In this particular situation, waves with wavelengths longer than those characterizing the cyclones will be strongly forced in the temperature field, since the modification should occur over at least the zonal length of the cyclone. A Fourier analysis of the resulting temperature field would indicate the development of waves with twice the length of the modified region. The spectrum forced in this manner would thus tend to have a strong component in the ultralong waves (wavenumbers 1–4) although this process should also affect other wavelengths. In less extreme situations, such as that shown in Fig. 4, forcing of the ultralong waves would also be expected due to the longitudinal variations of the eddy heat flux.

We can also qualitatively infer the structure of other fields of the ultralong waves forced in this manner. For example, we can apply the quasi-geostrophic omega equation to determine the vertical motion field. Averaging this equation longitudinally over the limited region that is modified by the eddy heat flux, we obtain

$$\sigma\nabla^2\bar{\omega} + \frac{f^2}{g}\frac{\partial^2\bar{\omega}}{\partial p^2} = \frac{f}{g}\frac{\partial}{\partial p}[\bar{\mathbf{V}}_g\cdot\nabla(\bar{\xi}_g + f)] + \frac{R}{gp}\nabla^2(\bar{\mathbf{V}}_g\cdot\nabla\bar{T}) + \frac{f}{g}\frac{\partial}{\partial p}\overline{(\mathbf{V}_g'\cdot\nabla\xi_g')} + \frac{R}{gp}\nabla^2\overline{(\mathbf{V}_g'\cdot\nabla T')},$$

where $\mathbf{V}_g$ is the geostrophic wind vector, ξ_g the vorticity of the geostrophic wind and σ a measure of static stability (see, e.g., Haltiner, 1971, p. 149 for more details). Here the overbar denotes a longitudinal average in the limited area and the prime a deviation from this average. A scale analysis of the terms on the right-hand side of this equation (Haltiner, 1971, p. 63) demonstrates that the first two terms are much smaller than the last two, because the longitudinally averaged meridional velocities are an order of magnitude smaller than the perturbation meridional velocities.

The last two terms in the above equation may be rewritten using the approximations

$$\overline{\mathbf{V}_g'\cdot\nabla\xi_g'} \approx \overline{\nabla\cdot\mathbf{V}_g'\xi'},$$

$$\overline{\mathbf{V}_g'\cdot\nabla T'} \approx \overline{\nabla\cdot\mathbf{V}_g'T'}.$$

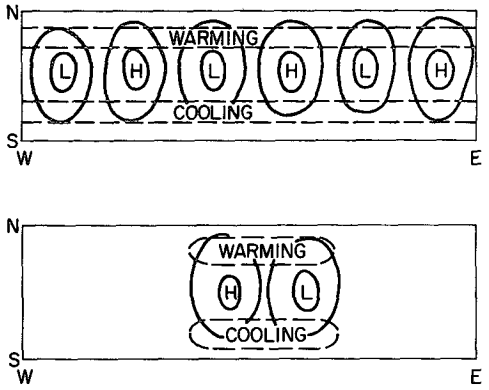

FIG. 5. Schematic diagram depicting the regions of warming and cooling due to the northward eddy heat flux from equally intense, equally spaced cyclones (upper figure) and from intense cyclones in only a portion of the zonal strip (lower figure). The solid lines denote surface pressure isobars.

In a growing baroclinic wave, $\mathbf{V}_g'$ and T' have a strong positive correlation while $\mathbf{V}_g'$ and ξ_g' tend to be uncorrelated. Hence, the dominant term on the right-hand side of the equation is the last one. Thus, mean upward motion will be forced in the region warmed by the converging eddy heat flux, and downward motion will be forced in the area cooled by the diverging eddy heat flux.

A positive correlation between the temperature and vertical velocity perturbations would therefore occur in the waves forced in this manner, and thus there would be a positive contribution to the energy budget of the wave by $C(n)$, the conversion of available potential energy to kinetic energy at wavenumber n. Furthermore, since the initial forcing is through thermal processes, we would expect that, at least initially, $C(n)$ would represent the main kinetic energy source. Finally, the vertical motions in the regions of converging and diverging eddy heat flux imply divergent flow near the surface, and therefore the production of vorticity, with cyclonic vorticity and lower pressure developing near the surface in the warmed regions, while anticyclonic vorticity and higher pressure develop in the cooled regions.

c. *Structure*

If the long waves are being forced early in the experiment by the process described above, then they should exhibit a characteristic structure. They should have a double maximum in the amplitude of geopotential ϕ_n and temperature T_n, where n denotes the spectral component. The maxima should appear north and south of the developing baroclinic waves, and there should be a 180° phase shift between the north and south maxima. The modification of the basic flow by the developing baroclinic wave occurs mainly north and south of the wave, in the regions where the divergence of the eddy heat flux is greatest. This property gives rise to the two maxima. The changes in ϕ and T north and south of the baroclinic waves should be of opposite sign, implying the phase shift. In addition, the two maxima should in large measure be confined to the lower troposphere. There the eddy heat flux of baroclinic waves is strongest, and when high-pressure areas are cold relative to their surroundings and low-pressure areas relatively warm, the intensity of these pressure systems decreases with height. Finally, the correlation between the vertical velocity variable ω_n and T_n should be negative and should display two maxima centered in the region where the amplitudes of T_n and ω_n are greatest. Fig. 6 shows the amplitude and phase angles of T and ϕ for wave 3, while Fig. 7 shows $\overline{\omega_n \alpha_n}$, where α is specific volume. These figures clearly display the structure described above.

3. Conclusions and speculations

If we regard the development of the portion of the kinetic energy spectrum between wavenumbers 5 and 20 as reflecting the development of cyclones around the hemisphere, then because the developing energy spectrum is broad and contains spikes, the cyclones will be of varying intensity around the hemisphere. In general, these cyclones will all transport heat northward, but the stronger cyclones will transport more than the weaker ones. Thus, the modification of the basic flow will not be uniform around latitude circles, and waves that are longer than the zonal scale of the individual cyclones will be forced. We have presented evidence that the ultralong waves (wavenumbers 1–4) in our experiments are initially forced in this way. In fact, this forcing mechanism for the ultralong waves apparently resulted in growth rates for the ultralong waves that exceeded the growth rates of the baroclinic waves (waves 5–20).

The significance of this mechanism for forcing the ultralong waves in the atmosphere is uncertain. The process presumably plays a role, as there are always cyclones of varying intensity around the hemisphere. Unfortunately, it seems likely that the waves forced in this manner would have a fairly complex structure, which might well be difficult to recognize in observational data. Furthermore, waves forced by this process derive much of their kinetic energy through the negative correlation of ω and T, so that it will be difficult to distinguish waves forced by the interaction between the cyclone-scale waves and the basic flow from those forced by classical baroclinic instability. However, the ultralong waves forced in this manner should show a distinct relation to events of strong cyclogenesis. For example, the phase of a developing ultralong wave should be clearly related to the location of cyclogenesis. It might be worthwhile to seek such associations by synoptic analysis of observations or of model simulations.

In the numerical experiment the longitudinal dependence of the effects of high wavenumber cyclogenesis is a matter of chance. In the actual Northern Hemisphere such dependence is clearly due to alternating continental and oceanic sectors, with vigorous storm development favored in the central and western oceans. The structure of the associated development in lower wavenumbers may be difficult to determine from data because the cyclogenesis occurs in regions of virtually no rawinsonde coverage.

There are other nonlinear processes associated with cyclones that can contribute to strongly forcing the ultralong waves. For example, when moisture was included in the experiment described

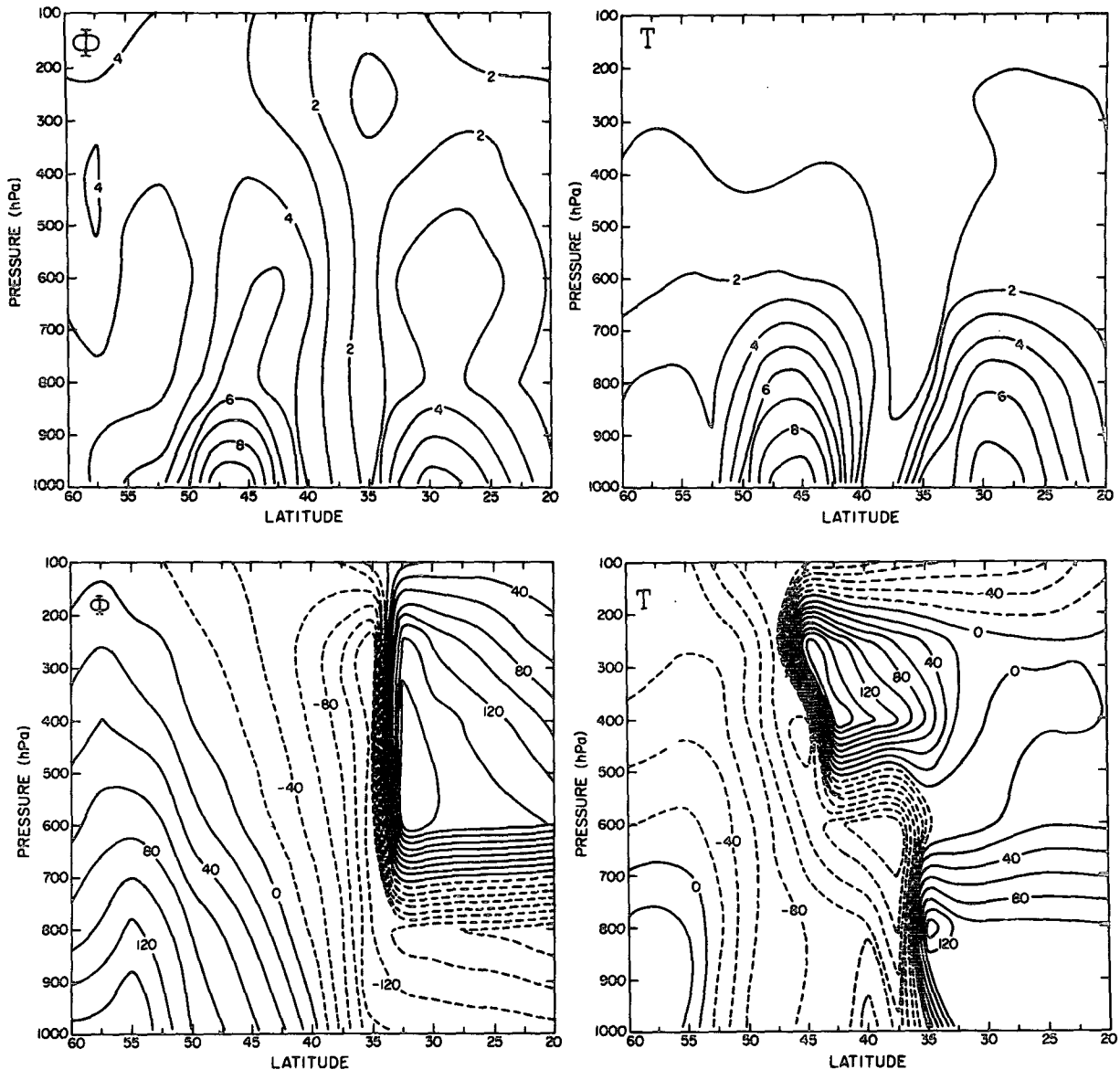

FIG. 6. Top row: zonal cross section of the amplitude of temperature T and geopotential ϕ for wave 3 at Day 15. The data have been normalized so that the maximum value is 10. Bottom row: cross section of the phase angle (deg) of temperature T and geopotential ϕ for wave 3 at Day 15.

by Gall (1976b), a few of the stronger cyclones became very intense relative to all the other cyclones around the channel. This was apparently caused by the release of latent heat within the cyclones. Because there were only a few widely spaced, very intense cyclones, a spectral analysis would indicate significant amplitude in the ultralong waves. Thus, in this way the ultralong waves can be forced by a very local process, the release of latent heat within the cyclone. In the moist experiment described by Gall (1976b), the ultralong waves grew from the beginning of the experiment while in the dry experiment, the development of the ultralong waves was delayed several days. We suspect that the growth of the ultralong waves early in the moist experiment was largely the result of the development of the few intense cyclones. Whether the waves forced in this manner should be considered waves in the physical sense or artifacts of the Fourier analysis is a moot point, but this process must also play a role in the energy budgets of some of the spectral components of the general circulation.

The ultralong wave forcing mechanism described here is simply a wave-wave interaction process and

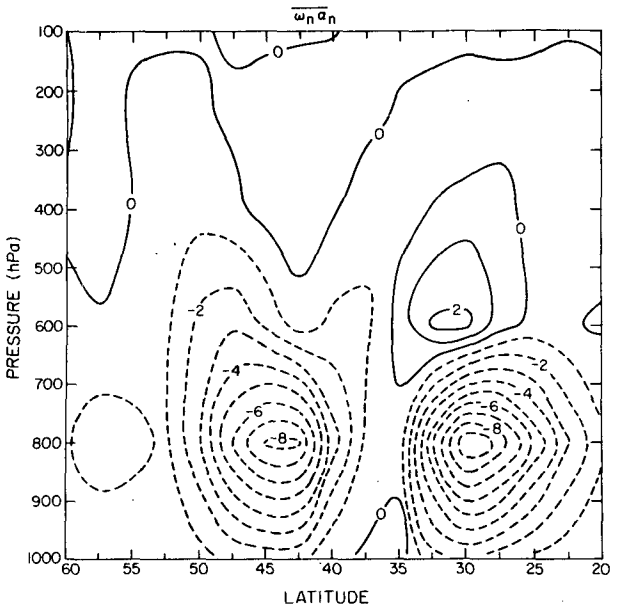

FIG. 7. Zonal mean cross section of $\overline{\omega_n \alpha_n}$ for wave 3 at Day 15. The data have been normalized so that the maximum value is 10.

thus should be included in any theory that accounts for energy sources for the ultralong waves through wave-wave interaction. However, to be complete, such a theory will ultimately have to take account of wave–wave interaction in both the kinetic energy and available potential energy budgets. Furthermore, this wave–wave interaction process might be very complicated and difficult to idealize. Perhaps the results presented here are indications that using Fourier series in this context to describe and follow the evolution of the eddies of middle latitudes is somewhat inappropriate in that the development of these eddies is essentially a local process. Trying to characterize such a local process using a spectrum involving global data may make the forcing and maintenance of the eddies appear unnecessarily complicated. A more useful viewpoint might be to consider the atmosphere as a collection of eddies (cyclones) developing and decaying locally and interacting only with their local basic flow and neighboring eddies.

If the process which we have described is important in the atmosphere, it may have significant implications for numerical weather prediction. Our arguments suggest that at least part of the forcing of the ultralong waves is directly from the cyclone-scale waves, and that this forcing can be very strong. Therefore, errors in numerical predictions of the ultralong waves may not necessarily be due to model deficiencies in the handling of ultralong wavelengths themselves, but rather to errors in the prediction of the cyclone scale.

Acknowledgments. This work was supported in part by the National Science Foundation under Contract ATM77-16047. The numerical experiments were conducted at the National Center for Atmospheric Research. The authors wish to thank Pat Downey for his assistance in preparing, running and analyzing the numerical experiments, Wayman Baker for the use of the energetics analysis programs, and Frederick Sanders for many useful comments.

REFERENCES

Baker, W. E., E. C. Kung and R. C. J. Somerville, 1977: Energetics diagnosis of the NCAR general circulation model. *Mon. Wea. Rev.*, **105**, 1384–1401.

——, —— and ——, 1978: An energetics analysis of forecast experiments with the NCAR general circulation model. *Mon. Wea. Rev.*, **106**, 311–323.

Brown, J. A., 1969: A numerical investigation of hydrodynamic instability and energy conversions in the quasi-geostrophic atmosphere. Part I. *J. Atmos. Sci.*, **26**, 352–365.

Charney, J. G., 1971: Geostrophic turbulence. *J. Atmos. Sci.*, **28**, 1087–1095.

Fjortoft, R., 1953: On the changes in the spectral distribution of kinetic energy for two-dimensional, nondivergent flow. *Tellus*, **5**, 225–230.

Gall, R. L., 1976a: A comparison of linear baroclinic instability theory with the eddy statistics of a general circulation model. *J. Atmos. Sci.*, **33**, 349–373.

——, 1976b: The effects of released latent heat in growing baroclinic waves. *J. Atmos. Sci.*, **33**, 1686–1701.

——, R. Blakeslee and R. C. J. Somerville, 1979: Baroclinic instability and the selection of the zonal scale of the transient eddies of middle latitudes. *J. Atmos. Sci.*, **36**, 767–784.

Haltiner, G. J., 1971: *Numerical Weather Prediction*. Wiley, 317 pp.

Hirota, I., 1968: On the dynamics of long and ultra-long waves in a baroclinic zonal current. *J. Meteor. Soc. Japan*, **46**, 234–249.

Kasahara, A., and W. M. Washington, 1971: General circulation experiments with a six-layer NCAR model, including orography, cloudiness and surface temperature calculations. *J. Atmos. Sci.*, **28**, 657–701.

Kraichnan, R., 1967: Inertial ranges in two-dimensional turbulence. *Phys. Fluids*, **10**, 1417–1423.

Lilly, D. K., 1969: Numerical simulation of two-dimensional turbulence. *Phys. Fluids*, Suppl. II, 240–249.

Oliger, J. E., R. E. Wellck, A. Kasahara and W. M. Washington, 1970: Description of the NCAR Global Circulation Model. NCAR Tech. Note TN-56, 94 pp.

Simmons, A. J., and B. J. Hoskins, 1977: Baroclinic instability on the sphere: Solutions with a more realistic tropopause. *J. Atmos. Sci.*, **34**, 581–588.

Song, R. T., 1971: A numerical study of the three-dimensional structure and energetics of unstable disturbances in zonal currents: Part II. *J. Atmos. Sci.*, **28**, 565–586.

Washington, W. M., and D. L. Williamson, 1977: A description of the NCAR global circulation models. *Methods in Computational Physics*, Vol. 17, J. Chang, Ed., Academic Press, 111–172.